Ecological Indicators 150 (2023) 110263

Contents lists available at ScienceDirect

Ecological Indicators

journal homepage: www.elsevier.com/locate/ecolind

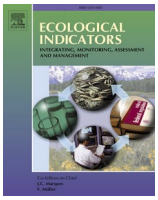

Interaction dynamics of multiple ecosystem services and abrupt changes of landscape patterns linked with watershed ecosystem regime shifts

Junyan Zhao [a], Jiajia Li [a], Lingli Zuo [a], Guohua Liu [b,c], Xukun Su [b,c,*]

[a] Institute of International Rivers and Eco-security, Yunnan University, Kunming 650091, China
[b] State Key Laboratory of Urban and Regional Ecology, Research Center for Eco-environmental Sciences, Chinese Academy of Sciences, Beijing 100085, China
[c] College of Resources and Environment, University of Chinese Academy of Sciences, Beijing 100049, China

ARTICLE INFO

Keywords:
Alternative stable states
Abrupt change
Tipping point
Nu-Salween River basin

ABSTRACT

Functional and structural regime shifts have been observed among many ecosystems. Understanding regime shifts in watershed ecosystems is crucial for landscape management and sustainable development. We propose the perspective that the relationship dynamics of ecosystem services (ESs) can reflect watershed ecosystem regime shifts. An assessment of the critical transitions in watershed landscape patterns is integrated to support the regime shift analysis. The downstream basin of the Nu-Salween River (NSR) was selected as the study area to demonstrate regime shifts occurring from 1999 to 2019. To detect the functional critical transition, changes in the relationships among various ESs, including in the habitat quality for biodiversity (HQ), carbon storage (CS), water yield (WY), soil conservation (SC) and grain production (GP), were revealed using time series correlation analysis. To identify the critical structural transitions of watershed, the Pettitt test and principal component analysis (PCA) were used to display changes in landscape patterns. The results showed that (1) WY and GP were key ESs that could define watershed stable states; (2) three states, the "coordinated state" from 1999 to 2008, the "transient state" from 2009 to 2013 and the "trade-off state" from 2014 to 2019, were identified in the downstream basin of the NSR; and (3) the watershed functional critical transition had a 1-year time lag with the structural critical transition. This research revealed the nonlinear dynamics of a complex system in watersheds, and the detection of regime shifts that integrate the interaction dynamics of ESs can better serve watershed management to cope with abrupt changes.

1. Introduction

Globally, the ecosystem state is affected by human activities and climate change (Sasaki et al., 2015). When an ecosystem suffers excess disturbances that are beyond its resilience capacity, an ecosystem state transition occurs (Suding and Hobbs, 2009). Multiple ecosystems can exhibit alternative stable states under certain environmental conditions (Scheffer et al., 2001). When ecosystems occur as alternative stable states, transitions between stable states often occur abruptly or suddenly (Kéfi et al., 2016). Human well-being may be further impacted by changes in ecosystem status by the ongoing provision of ecosystem services (ESs) (Biggs et al., 2018). The critical changes in ecosystem states are probably irreversible (Scheffer et al., 2001). Hence, for ecosystem management and sustainable development, it is essential to comprehend the changes in the state of ecosystem (Wu, 2013).

Regime shifts can be reflected in functional and structural ecosystem changes that are tremendous and often abrupt (Biggs et al., 2009). As nonlinear behaviors are widespread in ecosystems, internal variables often change nonlinearly when ecosystem regime shifts occur (Mayer and Rietkerk, 2004). Therefore, ecosystem indicator time series were employed to analysis whether abrupt change occur in ecosystem by a series of statistical methods (Andersen et al., 2009), including in marine (Tomczak et al., 2013b), grassland (Bestelmeyer et al., 2018), forest (Ospina et al., 2019), and urban ecosystems (Zhang et al., 2015). The recognition of tipping points among ecosystem indicators provides a common perspective for analyzing regime shifts. This method is widely used to detect social-ecological systems, natural ecosystems and social system shifts (Milkoreit et al., 2018). To avoid undesirable regime shifts, some statistical indicators have been developed as early warning signals. Abrupt increases in spatial correlation in a low-connectivity

* Corresponding author at: State Key Laboratory of Urban and Regional Ecology, Research Center for Eco-environmental Sciences, Chinese Academy of Sciences, Beijing 100085, China.
E-mail address: xksu@rcees.ac.cn (X. Su).

https://doi.org/10.1016/j.ecolind.2023.110263
Received 16 March 2023; Received in revised form 30 March 2023; Accepted 13 April 2023
Available online 22 April 2023
1470-160X/© 2023 The Author(s). Published by Elsevier Ltd. This is an open access article under the CC BY-NC-ND license (http://creativecommons.org/licenses/by-nc-nd/4.0/).

environment and in temporal autocorrelation in a high-connectivity environment can be applied to foretell regime shifts (Dakos et al., 2010). Likewise, when ecosystems approach the tipping point, the abnormal fluctuations among ecological and environmental variables can be early warning signals (Scheffer et al., 2012). However, the relationships between ecological components have not been taken into account in previous studies on regime shifts (Wu et al., 2020). Essential ecosystem functions can be represented by ecosystem services (ESs) that derived from ecosystems (De Groot et al., 2002). The interactions among ESs can shift through time when ecological processes change (Bennett et al., 2009). Different ESs can interact as trade-offs, or synergy (Jon Paul Rodriguez, 2012), or as neutral (Lee and Lautenbach, 2016). Quantifying the temporal characteristics of the ES relationship can create an opportunity to detect ecosystem regime shifts. On this basis, tipping point assessments of ecosystem structure are jointly employed to analyze whether ecosystem regime shifts occur. The components of ecosystems underpin the ecological processes that ultimately determine the provision of ESs (Fu et al., 2013). Landscape pattern evolution is directly linked to the dynamics of ecosystem structure (Ma et al., 2019). And landscape indices are useful to quantify landscape pattern at different levels (Tischendorf, 2001). We selected sets of landscape indices to estimate temporal changes in ecosystem structure at the landscape level. When ecosystem appear as alternative stable states, state variables will maintain stability within limits before and after tipping point (Beisner et al., 2003). The Pettitt Test is a sophisticated method for detection of tipping point in the mean value of indicators time series (Zhou et al., 2011). The fitted mean value of landscape indices can capture this important characteristic in alternative stable states. Therefore, Pettitt Test is adopted to investigate the time when a significant transition occurs in landscape indices; the transition is reflected in a shift in the ecosystem structural regime. Based on analysis of abrupt change of ecosystem function and structure, exploring whether watershed ecosystems can occur as alternative stable states is essential for watershed management. In addition, integrating the ES perspective into the study of the nonlinear dynamics of important ecological functional watershed ecosystems can provide insight into regional sustainability and human well-being..

We assume that in a stable ecosystem, the relationships among different ESs are perennially stable. When internal or external disturbances extend beyond ecosystem resilience, an ecosystem functional regime shift occurs, and the relationships of the ESs will change and stabilize again in the new phase. To test this hypothesis, we selected the downstream basin of the Nu-Salween River (NSR) as the study area to analyze abrupt changes among ES interactions and identify the alternative stable states within the watershed ecosystem. The NSR is one of the free-flowing rivers that still connect to the ocean in the world, exposing the sustained pressure faced by this watershed (Grill et al., 2019). As a transboundary river, the growing eco-security issues (e.g., species invasion, biodiversity losses) affect both China and neighboring countries (He et al., 2014). The downstream basin of the NSR is located in southwest China and is an ecological security shelter that supports biodiversity hotpot conservation (Su et al., 2022). Besides, the downstream basin of the NSR has a significant “corridor-barrier” function because its terrain is complicated and diversified, with deep canyons and high mountains (Yu et al., 2017). Moreover, the downstream basin of the NSR is the component of the Three Parallel Rivers of Yunnan Protected Areas, and most areas of this region are international ecological protection hotpots with sensitive and fragile ecosystems (Chen et al., 2019). In contrast to grazing in the upper reaches, the main agricultural activities are dry farming and irrigation farming in the downstream basin of the NSR, which serves as a key hub for the production of grains in western Yunnan Province (Chen et al., 2019). However, the quality of the vegetation in this region has decreased in recent decades (Huo and Sun, 2021). And the land cover has changed significantly, while the ecosystem service value has experienced variations, including a decrease and then an increase, in this important ecological functional area over decades (Wang et al., 2018).

In this study, we propose the perspective that the relationship dynamics of multiple ESs can reflect watershed ecosystem regime shifts. An assessment of the critical transitions of the watershed landscape pattern is integrated to support the regime shift analysis. The objectives of this study were (1) to identify the change of interactions between pairs of ESs from 1999 to 2019, (2) to detect the tipping point of landscape patterns and (3) to estimate the regime shifts of watershed ecosystems.

2. Materials and methods

2.1. Study area

The study area is a downstream basin of the NSR located in northwestern Yunnan Province, China (23°19′-28°12′N, 98°21′-100°12′E) (Fig. 1). The upper part of this region includes high mountain passes and valleys, where the topography is precipitous and narrow, and has a distinct “corridor-barrier” function and significant vertical climatic differences (Yang et al., 2021a,b). The bottom part of this region is relatively flat and contributes substantial grain production for Yunnan Province. The elevation ranges from 355 m to 5063 m. The annually precipitation is approximately 1336.7 mm, which is higher than the average level of Yunnan Province. The downstream basin of the NSR is an important part of the ecological corridor that links southern China and southeastern Asia (Wu et al., 2005). This region involves multiple of the ecosystem types present in the Northern Hemisphere, except deserts and oceans, and is a global gene reserve with extremely rich biodiversity (He et al., 2005).

2.2. Workflow and data collection

The workflow to estimate the regime shift of downstream basin of the NSR was shown in Fig. 2. Firstly, spatiotemporal distribution of ESs and time-series landscape pattern indices were quantified from 1999 to 2019. Secondly, Pettitt test analysis was used to detect abrupt change among two principal components of landscape pattern indices and average provision of ESs. Then, the interaction dynamics of multiple ESs were quantified through correlation analysis. On this basis, the regime shift of downstream basin of the NSR was estimated in function and structure two aspects to demonstrate our hypothesis. We acquired six types of data from 1999 to 2019 as Table 1 shown. The multisource observation data were appropriate for ESs mapping that by Integrated Valuation of Ecosystem Services and Tradeoffs (InVEST) software and assessment of landscape pattern that by Fragstats software.

2.3. ES assessment

We selected the key ESs on the strength of major ecological problems and the extremely low economic level of downstream basin of the NSR; we included habitat quality for biodiversity (HQ) as the support service; water yield (WY), soil conservation (SC) and carbon storage (CS) as the regulation services; and grain production (GP) as the provision service.

2.3.1. Grain production

Vegetation indices are often used for crop monitoring, and the NDVI has a linear correlation with grain production (Kuri et al., 2014). We chose the NDVI allocation method to calculate the GP within each arable land grid. The total grain output of Yunnan Province was extracted from the statistical yearbook. Then, the ratio of the time-series NDVI data within cultivated lands was associated with the grain output. The final results were clipped to our study area. The GP was calculated as follows:

$$GP_i = GP_{sum} \times \frac{NDVI_i}{NDVI_{sum}} \quad (1)$$

where GP_i is the output of grain products allocated to grid unit i, GP_{sum} is

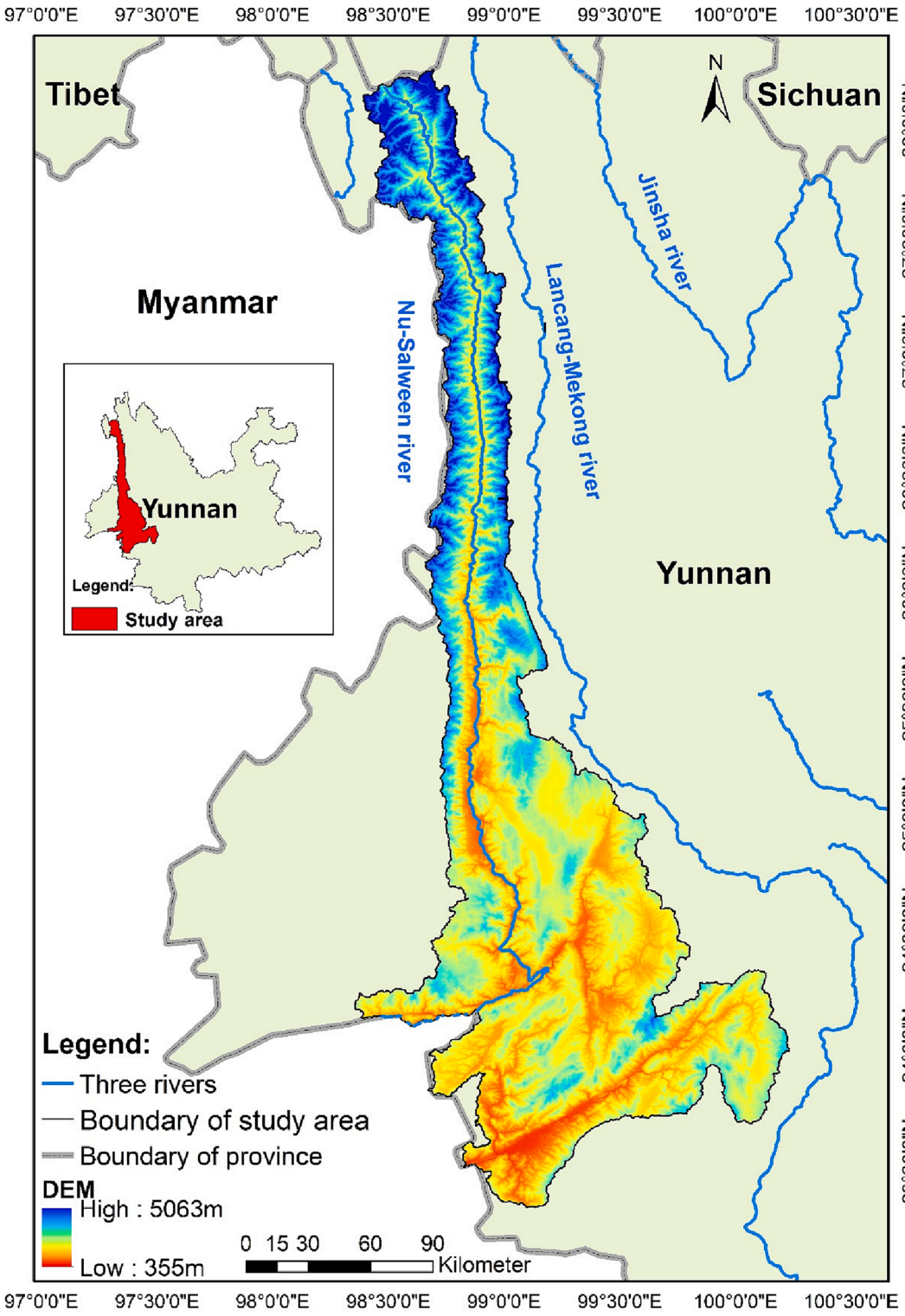

Fig. 1. Location of downstream basin of the NSR.

the total output of grain products, $NDVI_i$ is the normalized vegetation index of grid unit i, and $NDVI_{sum}$ is the sum of NDVI values for cultivated lands.

2.3.2. Carbon storage

The CS was assessed using the Carbon Model of the InVEST software. This model estimated CS via four carbon sinks that aboveground and belowground biomass, soil and dead organic matter (Sharp et al., 2018). The data required for the model were LULC and relevant carbon storage values for each LULC. The four carbon pools were obtained from the results of literature reviews (Terrado et al., 2016; Yang et al., 2018; Zhou et al., 2019). The CS was calculated as follows:

$$CS = C_{above} + C_{below} + C_{soil} + C_{dead} \quad (2)$$

where CS is the total carbon fixation supply (t/ha), C_{above} is the aboveground biochar, C_{below} is the underground biochar, C_{soil} is the organic

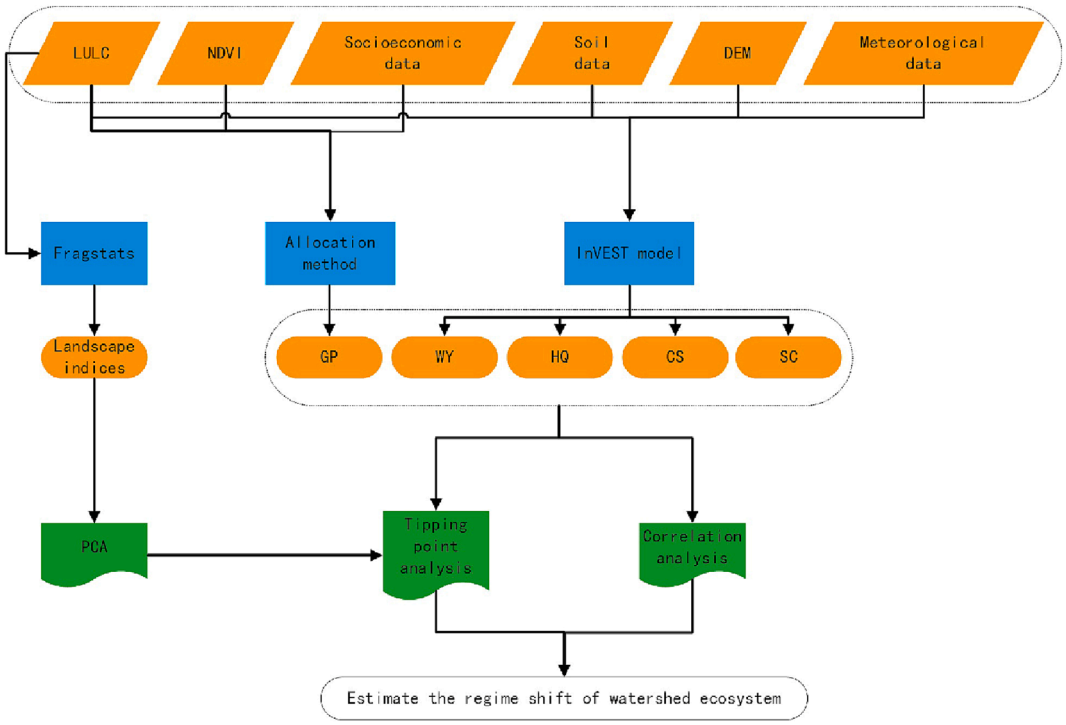

Fig. 2. The workflow chart for detecting the regime shift of downstream basin of the NSR.

Table 1
The data sources.

Data type	Data	resolution	Access	References
Land use and land cover (LULC)	wetland, barren, forest, impervious, cropland, snow/ice, shrub, water, and grassland	30 m	30 m annual land cover and its dynamics in China from 1990 to 2019 public domain at https://doi.org/10.5281/zenodo.4417810	(Yang and Huang, 2021)
Topography	ASTER GDEM data	30 m	Geospatial Data Cloud (http://www.gscloud.cn)	
Soil data	Soil property	1000 m	National Cryosphere Desert Data Center (https://www.ncdc.ac.cn)	
Meteorological data	Precipitation and temperature	1000 m	National Tibetan Plateau/Third Pole Environment Data Center (https://data.tpdc.ac.cn)	(Peng, 2020a, 2020b, 2020c)
Socioeconomic data	grain production	county	statistical yearbooks of Yunnan Province	
Vegetation data	normalized difference vegetation index (NDVI)	30 m	Resource and Environment Science and Data Center (http://www.resdc.cn)	

carbon in the soil, and C_{dead} is the dead organic carbon.

2.3.3. Water yield

The WY was assessed using the Water Yield Model of the InVEST software. Combined with precipitation and evaporation, this model estimated the water runoff in each grid and whole watershed respectively (Sharp et al., 2018). The data required for this model include plant available water content (*PAWC*), precipitation, DEM, soil depth, empirical constant (*Z* parameter), biophysical table data, watershed boundary and reference evapotranspiration (ET_0).

Both chemical and physical features of soil in China were applied to evaluate the PAWC (Zhou et al., 2005). The PAWC formula was expressed as follow:

$$PAWC = 54.509 - 0.132SAN - 0.003SAN^2 - 0.055SIL - 0.006SIL^2 - 0.738CLA + 0.007CLA^2 - 2.688C + 0.501C^2 \quad (3)$$

where *SAN*, *SIL*, *CLA*, and *C* are the proportions of sand, silt, clay, and organic matter in the soil (%), respectively.

The modified Hargreaves equation was utilized to calculate the annual ET_0 as proposed by Hargreaves and Allen. (2003). The Hargreaves equation is given as follows:

$$ET_0 = 0.0013 \times 0.408 \times RA \times (T_{av} + 17) \times (TD - 0.0123P)^{0.76} \quad (4)$$

where ET_0 is the reference evapotranspiration (mm/d), *RA* is the extraterrestrial radiation ($MJ \cdot m^{-2} \cdot d^{-1}$), T_{av} is the average of the mean daily maximum and mean daily minimum temperatures for each month, *TD* is the difference between the mean daily maximum and mean daily minimums for each month, and *P* is the precipitation per month.

Watersheds and subwatersheds were exacted by the ArcSWAT model based on the DEM. The watershed area covered the whole study area. The biophysical coefficients which model required were prepared in view of users' guide of the InVEST model and previous studies (Sharp et al., 2018; Wei et al., 2021; Yu et al., 2022). The *Z* parameter is a climate seasonality factor. Here, the default value was adopted (Borselli et al., 2008).

2.3.4. Soil conservation

The SC was assessed using the Sediment Delivery Ratio Model of the InVEST software. Combined with potential soil erosion and actual soil loss, this model estimated the sediment retention using the revised universal soil loss equation (RUSLE) and required LULC, DEM, rainfall erosivity (R), soil erodibility (K) and watershed boundary data. R was calculated using the empirical formula put forward by Wischmeier as follows:

$$R = \sum_{i}^{12} 1.735 \times 10^{\left[\left(1.5\times\log_{10}\frac{P_i^2}{P}\right)-0.8188\right]} \quad (5)$$

where R is the rainfall erosivity, MJ•mm/(ha•hr•yr); P_i is the monthly precipitation (mm/month); and P is the annual precipitation (mm/year).

K is the soil erodibility and was calculated using the erosion productivity impact calculator (EPIC) model (Williams et al., 1984) as follows:

$$K = \left\{0.2+0.3exp\left[0.256SAN\left(1-\frac{SIL}{100}\right)\right]\right\} \times \left(\frac{SIL}{CLA+SIL}\right)^{0.3} \times \left(1-\frac{0.25C}{C+exp(3.72-2.95C)}\right) \times \left(1-\frac{0.7(1-SAN)}{(1-SAN)+exp[2.29(1-SAN)]-5.51}\right) \quad (6)$$

where SAN, SIL, CLA, and C are the percent proportions of sand, silt, clay, and organic matter in the soil, respectively.

2.3.5. Habitat quality for biodiversity

The HQ was assessed using the Habitat Quality Model of the InVEST software. This model estimated HQ by analyzing LULC and threats. The threat sources included farmland and city settlement. The data required for the model were LULC and threat data which represent human-dependent influences include farmland and city settlement (in text and raster format).

2.4. Ecosystem regime shift detection

2.4.1. Correlation analysis

The values of multiple ESs within grids were exacted to points. Then, the relationships between pairs of ESs were identified by Pearson's test from 1999 to 2019. When the correlation coefficients and significance test changed in a specific year and continued to be stable after that year, it was assumed that that year was the tipping point of the ecosystem function that caused the ES interactions to transition to different phases.

2.4.2. Principal component analysis

Correlated time-series data that reflect ecosystem states can be compressed using principal component analysis (PCA) (Möllmann et al., 2009). Here, we used the PCA method to quantify the transformed values and contributions of time-series landscape indices in two components (i.e. PC1 and PC2). Ten landscape indices (Table 2) were selected to estimate regional landscape patterns (i.e. watershed ecosystem structure) from 1999 to 2019 in shape, aggregation and diversity aspects. The yearly scores of PC1 and PC2 were extracted against years for subsequent step.

2.4.3. Pettitt test analysis

The rank-based nonparametric statistical test method called Pettitt test analysis was applied to detect abrupt changes (Pettitt, 1979). The yearly PC1 and PC2 scores were analyzed by the Pettitt test to detect whether and when abrupt changes had occurred. Additionally, yearly ES mean grid provisions were analyzed to identify tipping points. The Pettitt test is expressed as follows:

Table 2
Selection of landscape indices (Jaeger, 2000; McGarigal and Marks, 1995).

Landscape indices	Description
Mean perimeter-area ratio (PARA_MN)	The average ratio of the patch perimeter to area, reflecting complexity of landscape shape
Continuity index (CONTIG)	The spatial connectedness of patch shape, the higher the CONTIG the higher the adjacency of patch.
Mean shape index (SHAPE_MN)	The average patch shape for all patches in landscape, reflecting complexity of landscape shape
Landscape shape index (LSI)	A perimeter-to-area quantify the amount of edge present in landscape, reflecting complexity of landscape shape
Patch density (PD)	The number of patches per unit area, reflecting fragmentation of landscape
Splitting index (SPLIT)	The number of patches that landscape is divided into same DIVISION with a constant patch size
Patch cohesion index (COHESION)	The physical connectedness of the corresponding patch type
Landscape division index (DIVISION)	The probability that two selected places are not locate in one patch of landscape. The higher the DIVISION the higher landscape fragmentation
Shannon's diversity index (SHDI)	The amount of "information" per patch that is based on information theory, reflecting heterogeneity of landscape
Shannon's evenness index (SHEI)	The relative abundance of patch types, reflecting evenness of landscape

$$U_{t,T} = \sum_{i=1}^{t}\sum_{j=t+1}^{T} sgn(x_j - x_i), 1 \le t < T \quad (7)$$

where

$$sgn(\theta) = \begin{cases} 1 if \theta > 0; \\ 0 if \theta = 0; \\ -1 if \theta < 0. \end{cases} \quad (8)$$

The test statistic $U_{t,T}$ can also be obtained by the following recursive relation when the series has a continuous distribution.

$$U_{t,T} = U_{t-1,T} + V_{t,T} \quad (9)$$

For $t = 2,\ldots,T$, where

$$V_{t,T} = \sum_{j=1}^{T} sgn(x_j - x_t) \quad (10)$$

and

$$U_{1,T} = V_{1,T} \quad (11)$$

The most likely change point, τ, is found to satisfy the following criteria:

$$K_\tau = |U_{\tau,T}| = max|U_{t,T}| \quad (12)$$

The significance probability p is evaluated as follows:

$$p = 2\exp\left(\frac{-6K_T^2}{T^2+T^3}\right) \quad (13)$$

2.4.4. Heatmap analysis

Heatmap analysis is helpful to visualize time series patterns which may contain abundant indicators (Tomczak et al., 2013a). Ten landscape indices were normalized and plotted by five levels to visualize the temporal patterns.

3. Results

3.1. Spatiotemporal patterns and provision of multiple ESs

The distribution of multiple ESs was mapped to analyze the dynamics of the spatial pattern (Appendix Figure S1). From 1999 to 2019, the

overall spatial pattern of multiple ESs remained steady. At the grid level, each ES did not exhibit any significant spatial clustering property. The mean, maximum and minimum WY values were 283.65 mm, 2103.22 mm (in 2016) and 6 mm (in 2014), respectively. The mean provisions of HQ, CS, GP, and SC were 0.9021, 13.48 kg/km^2, 36.68 kg/km^2, and 350.24 kg/km^2 over 21 years, respectively. The maximum mean HQ was 0.9021 in 1999, and the minimum mean HQ was 0.8985 in 2018. The maximum mean CS was 13.58 kg/km^2 in 2011, and the minimum mean CS was 13.40 kg/km^2 in 2018. The maximum mean GP was 44.48 kg/km^2 in 2018, and the minimum mean GP was 28.92 kg/km^2 in 1999. The maximum mean SC was 526.37 kg/km^2 in 2016, and the minimum mean SC was 238.31 kg/km^2 in 2018. The spatial distributions of WY, HQ and CS were highly similar in the southern study area, where a high provision of GP was mainly located.

The fitted average provision of regulation services decreased while provision service increased after abrupt changes, meaning that potential trade-offs occurred between regulation and provision services after regime shifts, as shown in Fig. 3(a-d). The tipping points of WY and GP, CS and HQ were the same, which were identified in 2008 and 2012, respectively. Therein, WY and GP exhibited consistency with abrupt changes in the landscape (see Fig. 3a, 3b and Fig. 6b). Relative to the provision of ESs that fluctuate randomly (i.e. SC, see Appendix Figure S2) or consistently but the interaction was always stable (i.e. CS and HQ, see Fig. 3c, 3d and Fig. 4), WY and GP might be the key ESs linked with ecosystem states.

3.2. Interactions among multiple ESs

From 1999 to 2019, there were 193 pairs of ESs among 210 possible pairs that were high correlation (Fig. 4(a-u)). The interactions of WY-HQ, WY-CS, HQ-CS, HQ-GP, HQ-SC, CS-GP, CS-SC, and GP-SC were stable except in 2001 and 2003, when the Pearson correlation coefficients (r) of HQ-GP and CS-GP were$<$0.1. The mean r values among the 8 stable interactions of pairs of ESs were −0.52, −0.56, 0.97, 0.29, 0.40, 0.34, 0.38, and 0.26 during the study period. The interaction between WY and SC fluctuated randomly with a weakly positive correlation or neutral correlation apart from the negative correlation found in 2015 ($r < 0.1$). The relationship between WY and GP appeared to be positively correlated from 1999 to 2008, except in 2005. However, from 2009 to 2013, this relationship changed frequently. Since 2014, this relationship had a steady strong negative correlation ($r <$ -0.2 and $p <$ 0.001). According to the dynamic change in the interaction between WY and GP, a regime shift in ecosystem function occurred compared with synergy in the previous ecosystem state, which ranged from 1999 to 2008. GP exhibited a trade-off with WY in the new ecosystem state.

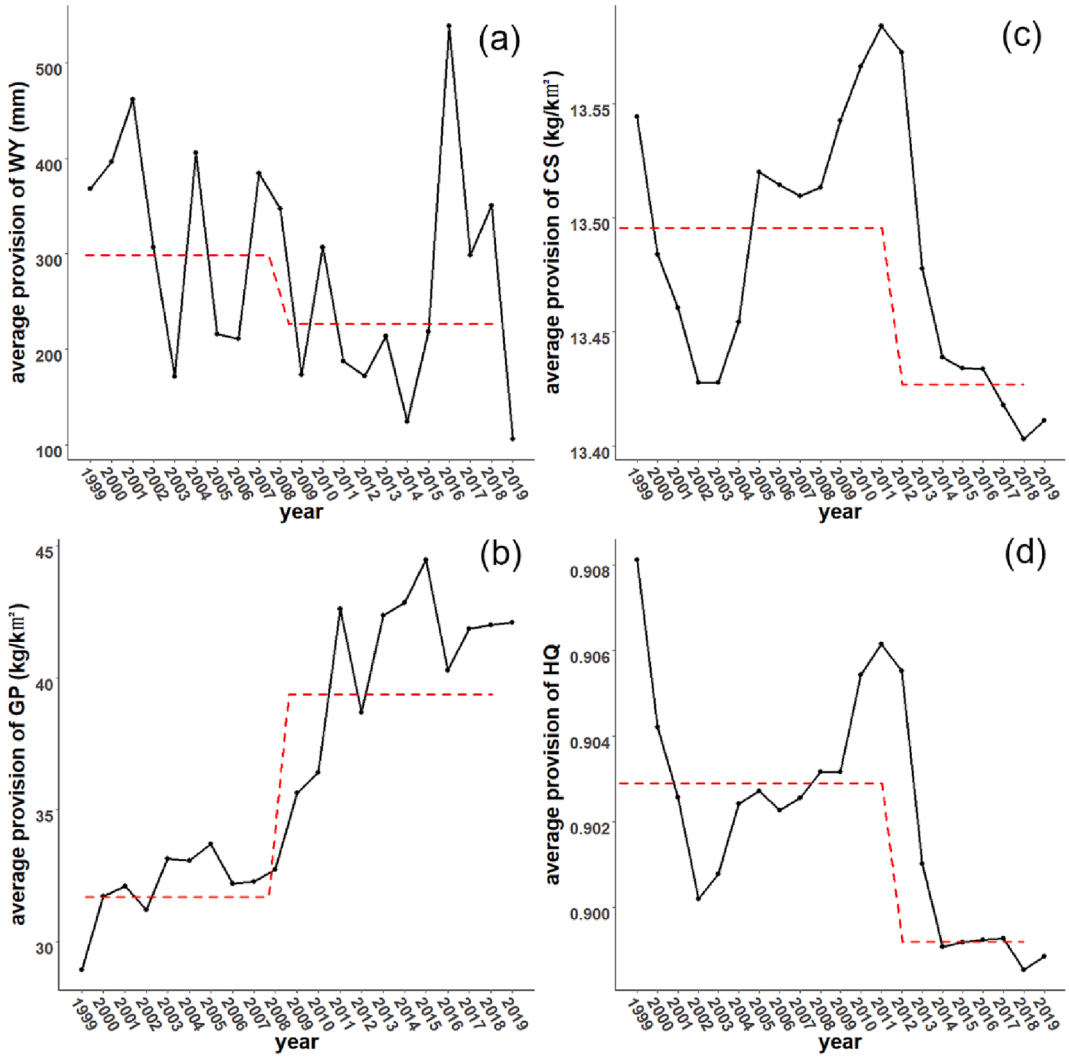

Fig. 3. Tipping point for the average provision of each ES. Panels (a)-(c) represent the Pettitt test results for a change in the mean in the time series to the provision of CS ($p < 0.05$), WY ($p < 0.5$) and GP ($p < 0.05$), respectively; the fitted mean provision before and after the tipping point is depicted by the red dotted lines. (For interpretation of the references to color in this figure legend, the reader is referred to the web version of this article.)

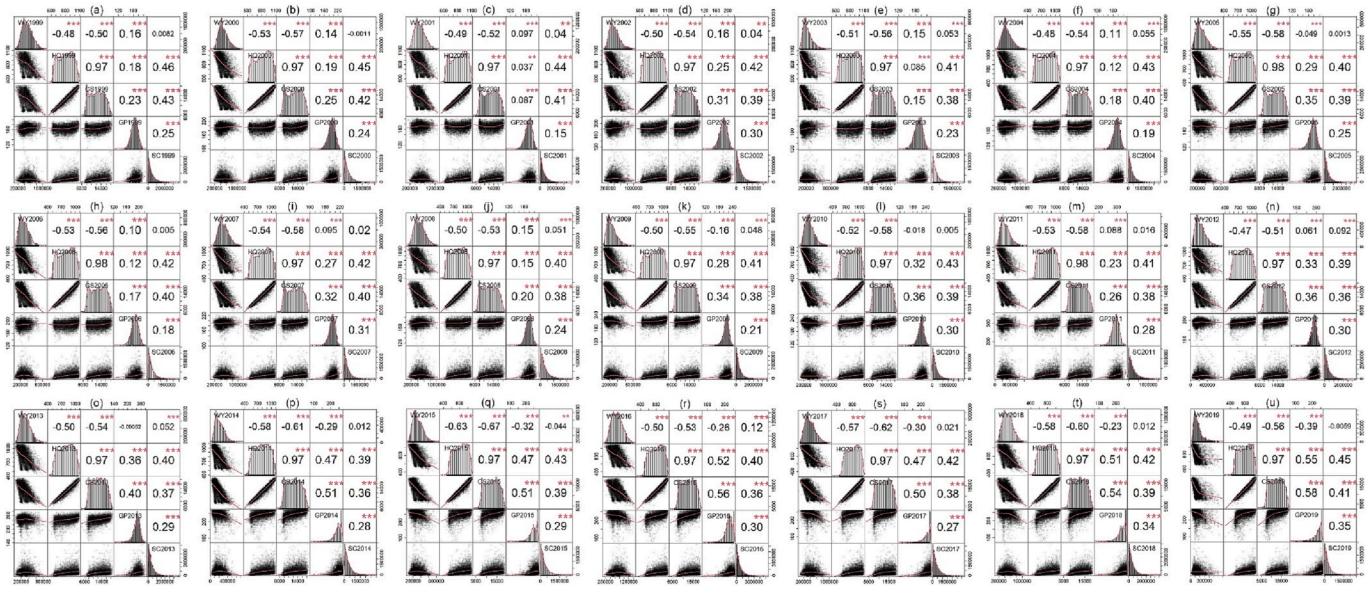

Fig. 4. Pearson correlation coefficients between ES pairs against years. Significant correlations are represented by labels * ($p < 0.05$), ** ($p < 0.01$), *** ($p < 0.001$).

3.3. Landscape pattern changes

As shown in Fig. 5, PC1 and PC2 could explain 93.3% of all landscape indices. The first axis was mainly correlated with the COHESION, DIVISION, SHDI and SHEI terms. The second axis was mainly correlated with the LSI, PD, PARA_MN and CONTIG terms. That is, PC1 reflected the characteristics of contagion/interspersion and diversity within the landscape, while PC2 reflected the characteristics of shape, area and density within the study area.

The features of the COHESION, DIVISION, SPLIT, SHEI and SHDI trends were similar and could be divided into three phases, ranging from 1999 to 2007, from 2008 to 2012, and from 2013 to 2019 (see Fig. 6). Since 2013, the characteristics of all landscape indices have been immeasurable in contrast to previous values. The Pettitt test detected tipping points of PC1 scores and PC2 scores in 2013 and 2008, respectively. The results of the tipping points indicated that the density, shape and area of the regional landscape were simpler after 2008 and the heterogeneity and fragmentation of the regional landscape increased after 2013. The landscape pattern of the downstream basin of the NSR experienced transformation from 2008 to 2012. The landscape pattern transitions converted to a different phase across the tipping point in 2013. There was a 5-year lag between abrupt changes in the integral structure of the watershed ecosystem and the shape and density changes in the landscape pattern.

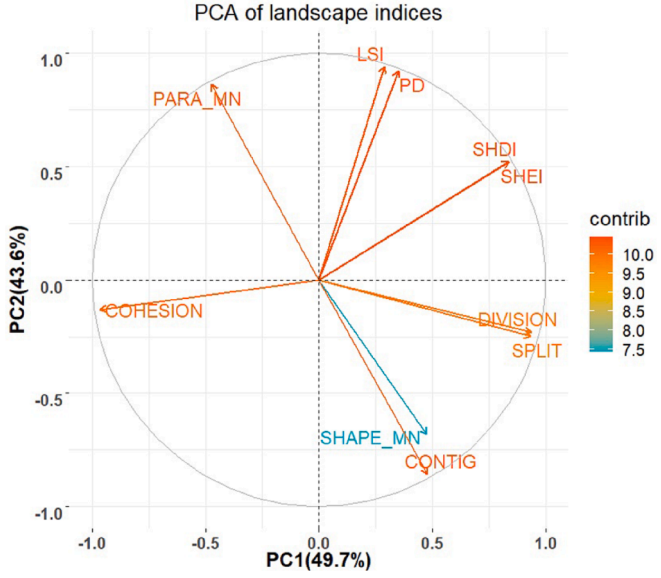

Fig. 5. The dependencies of variables from PCA. The gradient color of each arrow represents the contributions of landscape indices to the PCs. The correlation circles represent the correlations between each landscape index and the two principal components.

4. Discussion

4.1. Watershed ecosystem regime shift

The uniformity of presentation among ES interactions and landscape patterns across tipping points shows that the regional ecosystem functions and spatial structures transitioned to other phases, indicating that the downstream watershed ecosystem of the NSR basin underwent a regime shift in 2014. For ecosystem function, we identified two stable phases, the provision-regulation service coordinated phase (from 1999 to 2008) and the provision-regulation service trade-off phase (from 2014 to 2019), based on the time-series correlation analysis results. In the coordinated phase, the WY was synergistic with the GP, although the correlation coefficient ($0.1 < r < 0.2$) was lower than the other 8 stable pairs of ESs (mean $|r|$ range from 0.26 to 0.97) during most of the period. This result can be considered a win–win outcome for decision makers who are concerned with regulation services and local farmers who focus on agricultural incomes. It is important to note that although WY and GP have a positive correlation at the spatial scale, the average provision of GP is significantly lower than the average level in this phase (Fig. 3). In the trade-off phase, the relationship of WY and GP was opposite, while the correlations of the other ESs did not change significantly. Ecological restoration, such as forestation, can reduce WY after a time lag (Li et al., 2021), so the long-term effects of the two world's largest ecological restoration programs (the Natural Forest Conservation Program and the Sloping Land Conversion Program), which launched over two decade and covered most of China (Ouyang et al., 2016), may be potential incentives for regional ecosystem regime shifts.

Regarding the ecosystem structure, the dynamics of landscape indices indicate that there are also two stable phases: the complexity and aggregation phase (from 1999 to 2007) and the simplicity and fragmentation phase (from 2013 to 2019). Landscape patterns are strongly

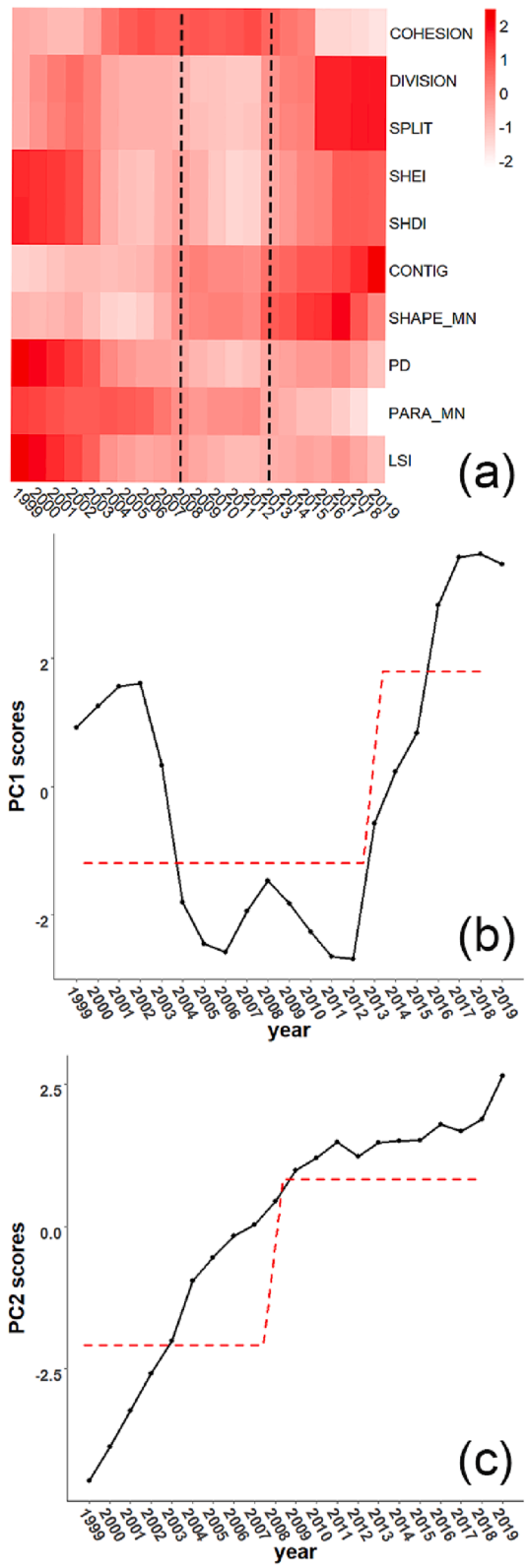

Fig. 6. Heatmap of landscape indices and Pettitt test results of the PC1 ($P < 0.5$) and PC2 ($P < 0.01$) scores against the years. The gradient colors of the grids representing the z score values of landscape indices (a), (b) and (c) represent the Pettitt test results indicating a change in the mean value to PC1 and PC2 scores, respectively, with the red dotted lines representing the fitted mean principal component scores before and after the tipping point. (For interpretation of the references to color in this figure legend, the reader is referred to the web version of this article.)

correlated with the provision of hydrological ESs within watershed ecosystems (Yohannes et al., 2021). This correlation could be reflected in the synchronism of abrupt changes in the average provision of WY and landscape indices (Fig. 3 and Fig. 6). However, there is an inconformity between the critical transition of ecosystem function and ecosystem structure, suggesting that the ecosystem structure shift is antecedent to the ecosystem function shift 1 year within the downstream basin of the NSR. Composite considered the different stable phases of ecosystem function and structure, the watershed ecosystem was divided into alternative stable states: the "coordinated state" from 1999 to 2008 and the "trade-off state" from 2014 to 2019. Furthermore, we detected an early warning signal both in the ecosystem function and structure. Regulation services can usually define a ecosystem regime with influencing ecosystem resilience while other ESs not change (Bennett et al., 2009). Likewise, before a regime shift occur, a particular spatial pattern would be generated (Scheffer et al., 2009; Dai et al., 2013). At 6 years before the ecosystem function transition, the average provision of WY decreased to a relatively low level, which may have led to the resilience of ecosystem decline. This change could result in ecosystems becoming sensitive to disturbances. Moreover, the abrupt changes in the shape and density of the landscape in 2008 can be a warning signal that the ecosystem structure is unstable. These results indicate that the ecosystem is on the verge of regime shift. According to the fluctuations among the interactions of pairs of ESs and landscape patterns, the period from 2008 to 2013 was the transition period of the ecosystem state (i.e. "transient state"). Hysteresis was also observed in the transition period: abnormal fluctuations in the correlation between WY and GP had a 1-year lag to abrupt changes in PC2 of landscape patterns and the provision of WY and GP in 2008; the abrupt changes of average provision of CS and HQ also had a 1-year lag to abrupt changes in PC1 of landscape patterns in 2012.

The ecosystem state is closely related to human activities and climate change (Rietkerk et al., 2004). Extreme weather is a significant external disturbance to ecosystems. From 2009 to 2010, Yunnan Province suffered an extreme drought that lasted 237 days (Li et al., 2015). This extreme event led to a change in the WY, which may have been the trigger of the watershed ecosystem regime shift. Moreover, GP and climate change play important roles in driving regime shifts, which may generate cascading regime shifts (Rocha et al., 2015). Therefore, guaranteeing sufficient redundancy of capacity for the provision of GP within watershed ecosystems can guard effectively against unexpected regime shifts.

4.2. Implications for watershed management

Identifying regime shifts can help to cope with large and abrupt changes in ecosystems. However, environmental variables (e.g., biological, anthropogenic and climate variables) have been focused in majority of regime shift studies, while ESs few have taken into consideration (Bi et al., 2021). The integration of ES perspectives into ecosystem regime shifts is a fair effort to better support the sustainable watershed ecosystems management. Ecosystem states are closely related to ESs that ultimately impact human well-being (Crépin et al., 2012). However, sometimes transition of ecosystem state did not affect provision of ESs because of ecological robustness (Hautier et al., 2015; Mumby et al., 2014). Our findings noted in Fig. 7 show that the patterns of ESs do not appear significant changes before and after watershed ecosystem cross tipping point except GP. In other words, watershed ecosystem regime shift was likely ES pattern-free. Hence, in watershed management, focusing on interaction and provision level rather than heterogeneity of ESs might facilitate capture ecosystem dynamic state.

ESs have a strong link with sustainable development goals (SDGs) from the regional to the global level (Yang et al., 2020). Watersheds are a natural unit of terrestrial ecosystems, and their unique ecological processes generate sets of ESs that contribute to the SDGs. Hence, obtaining precise descriptions of ecosystem state shifts based on the ES

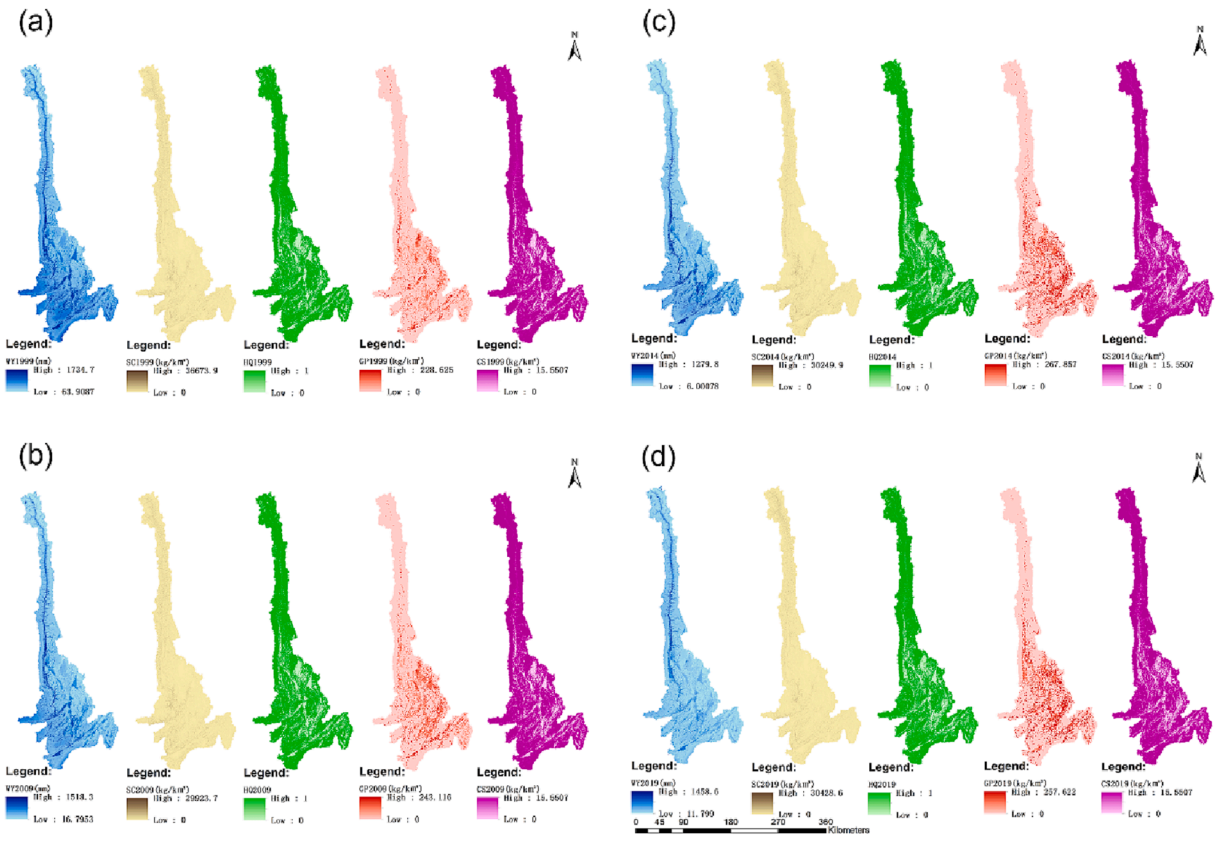

Fig. 7. Spatial patterns of multiple ESs before and after regime shift. (a) represent spatial pattern of ESs at the beginning of the study period in 1999; (b) at the beginning of "transient state" in 2009; (c) at the time ecosystem cross tipping point in 2014; (d) at the end of the study period in 2019.

approach in watershed ecosystems can advance our ability for ecosystem management toward the SDGs.

The five ESs (WY, HQ, GP, CS and SC) that are estimated in this study have critical links to SDG1, SDG2, SDG3, SDG6, SDG13 and SDG15, that is, No Poverty, Zero Hunger, Good Health, Clean Water, Climate Action and Life on Land. Thereof, SDG2, SDG1 and SDG6 are recognized as top priorities at both the regional and global levels (Yang et al., 2020). The WY and GP are deemed core ESs that provide abrupt changes in accordance with landscape patterns, which can define the ecosystem state. WY and GP are perceived to have strong levels of support for contributing to the achievement of the 25 and 28 SDG targets, respectively (Wood et al., 2018). Food security is underpinned by the GP, which highly competes with WY in general (Liu et al., 2022; Mohammadi et al., 2021). After the regime shift, the ecosystem enters the trade-off phase in which WY competes with GP significantly, thus impeding the achievement of the SDGs. Ecosystem condition transitions are probably irreversible (Scheffer et al., 2001), and provision services usually trade off with regulation services on account of human demands (Pan et al., 2014). To mitigate the trade-off between WY and GP in the trade-off phase, better management of croplands, advanced agricultural production and water-saving techniques are feasible (Fu et al., 2022). Changes in cultivated lands, planting densities, fertilization and modern crop varieties all impact the provision of GP (Yang et al., 2021a,b). Afforestation promotes regional vegetation, which contributes to a decrease in WY through canopy evapotranspiration (Ellison et al., 2012). The abrupt decline in the WY provision may be associated with afforestation activities and the increase in agricultural water utilization that underpin the abrupt addition of the provision of the GP. Therefore, the extent and proportion of ecological restoration and agricultural production within watersheds should give sufficient consideration to temporal accumulation to mitigate the probable trade-off of ESs after regime shifts. The balance between environmental protection and socioeconomic development is a long-term management objective in the downstream basin of the NSR. Additionally, the contribution of ESs to SDG achievement is a long-term process that depends on the natural resource endowment and background of local ecosystems that maintain the provision of the ESs (Xu et al., 2022). Hence, long-term watershed management objectives that take into account the abrupt changes in interactions among ESs are essential for ensuring the long-term sustainability provision of ESs. Long-term watershed ecosystem management objectives should be combined to fit the time scale of regime shifts that often suffer persistent pressures over decades (Tomczak et al., 2013a).

Moreover, the transition period (from 2008 to 2014) creates an undesired regime shift. The emergent abnormal fluctuations and patterns within ecosystem functions and structures in this period imply that the ecosystem state appears less stable. Appropriate management interventions are practicable to escape this transient period and direct the ecosystem forward or backward to a stable state (Francis et al., 2021). The joint adoption of mitigation and adaptation strategies is wise before a potential regime shift occurs (Crépin et al., 2012). In this study, when intervening measures can mitigate the fluctuation in the interaction between WY and GP, mitigation strategies should be applied prior to adaptation strategies. When adaptation strategies can preferably progress to achieve the watershed SDGs in the trade-off phase, mitigation strategies may not be necessary. Therefore, watershed managers should consider ecosystem states in stable and transient phases simultaneously to better deal with presently occurring and forthcoming regime shifts.

5. Conclusion

In this research, the interaction dynamics of ESs were verified to reflect regime shifts in the downstream basin of the NSR. WY and GP were identified as core ESs that can define the states of the downstream

basin of the NSR through time-series correlation analysis and tipping point methods. The results demonstrated that the regional ecosystem state in the downstream basin of the NSR had transferred to another phase in 2014. This regime shift had a 6-year delay with early warning signals: the PC2 of landscape patterns and the average provisions of WY and GP simultaneously changed abruptly in 2008. Moreover, the abrupt transition of ecosystem structure occurred prior to the abrupt transition of ecosystem function with a 1-year interval. This hysteresis was also observed in ESs in which the abrupt transition among the average provision of WY and GP occurred prior to the abnormal fluctuations in the interaction between WY and GP. Our findings indicated that the downstream basin of the NSR ecosystem exhibited alternative stable states, including a "coordinated phase" from 1999 to 2008 and a "trade-off phase" from 2014 to 2019. In addition, there was a "transient phase" during which the downstream basin of the NSR ecosystem was close to the tipping point and lost resilience between the two stable states from 2009 to 2013. These results provide a foundation to cope with unexpected critical changes in watershed ecosystems. Furthermore, the integration of the interaction dynamics of ESs that bridge social systems and ecosystems with regards to regime shifts can be applied to navigate sustainable watershed management directly.

CRediT authorship contribution statement

Junyan Zhao: Conceptualization, Software, Writing – original draft, Visualization, Data curation. **Jiajia Li:** Data curation. **Lingli Zuo:** Data curation. **Guohua Liu:** Conceptualization, Methodology. **Xukun Su:** Conceptualization, Methodology.

Declaration of Competing Interest

The authors declare that they have no known competing financial interests or personal relationships that could have appeared to influence the work reported in this paper.

Data availability

Data will be made available on request.

Acknowledgments

We thank all people involved for helping us complete the research. This study was supported by the Second Tibetan Plateau Scientific Expedition and Research Program (STEP) under grant no. 2019QZKK0402. The meteorological dataset was provided by the National Tibetan Plateau Data Center (http://data.tpdc.ac.cn).

Appendix A. Supplementary data

Supplementary data to this article can be found online at https://doi.org/10.1016/j.ecolind.2023.110263.

References

Andersen, T., Carstensen, J., Hernandez-Garcia, E., Duarte, C.M., 2009. Ecological thresholds and regime shifts: approaches to identification. Trends Ecol. Evol. 24, 49–57.

Beisner, B.E., Haydon, D.T., Cuddington, K., 2003. Alternative stable states in ecology. Front. Ecol. Environ. 1, 376–382. https://doi.org/10.1890/1540-9295(2003)001[0376:ASSIE]2.0.CO;2.

Bennett, E.M., Peterson, G.D., Gordon, L.J., 2009. Understanding relationships among multiple ecosystem services. Ecol. Lett. 12, 1394–1404. https://doi.org/10.1111/j.1461-0248.2009.01387.x.

Bestelmeyer, B.T., Peters, D.P.C., Archer, S.R., Browning, D.M., Okin, G.S., Schooley, R. L., Webb, N.P., 2018. The grassland-shrubland regime shift in the southwestern United States: Misconceptions and their implications for management. Bioscience. 68, 678–690. https://doi.org/10.1093/biosci/biy065.

Bi, J., Hao, R., Li, J., Qiao, J., 2021. Identifying ecosystem states with patterns of ecosystem service bundles. Ecol. Indic. 131, 108195 https://doi.org/10.1016/j.ecolind.2021.108195.

Biggs, R., Carpenter, S.R., Brock, W.A., 2009. Turning back from the brink: Detecting an impending regime shift in time to avert it. Proc. Natl. Acad. Sci. 106, 826–831. https://doi.org/10.1073/pnas.0811729106.

Biggs, R., Peterson, G.D., Rocha, J.C., 2018. The regime shifts database: A framework for analyzing regime shifts in social-ecological systems. Ecol. Soc. 23 https://doi.org/10.5751/ES-10264-230309.

Borselli, L., Cassi, P., Torri, D., 2008. Prolegomena to sediment and flow connectivity in the landscape: A GIS and field numerical assessment. Catena. 75, 268–277. https://doi.org/10.1016/j.catena.2008.07.006.

Chen, W., Xu, J., Li, S., 2019. A Study on the Characteristics of Hydrological and Meteorological Droughts in the Lower Nu River. Nat. Univ. Pekin. 55, 764–772. https://doi.org/10.13209/j.0479-8023.2019.034.

Crépin, A.S., Biggs, R., Polasky, S., Troell, M., de Zeeuw, A., 2012. Regime shifts and management. Ecol. Econ. 84, 15–22. https://doi.org/10.1016/j.ecolecon.2012.09.003.

Dai, L., Korolev, K.S., Gore, J., 2013. Slower recovery in space before collapse of connected populations. Nature. 496, 355–358. https://doi.org/10.1038/nature12071.

Dakos, V., van Nes, E.H., Donangelo, R., Fort, H., Scheffer, M., 2010. Spatial correlation as leading indicator of catastrophic shifts. Theor. Ecol. 3, 163–174. https://doi.org/10.1007/s12080-009-0060-6.

De Groot, R.S., Wilson, M.A., Boumans, R.M.J., 2002. A typology for the classification, description and valuation of ecosystem functions, goods and services. Ecol. Econ. 41, 393–408. https://doi.org/10.1016/S0921-8009(02)00089-7.

Ellison, D., Futter, M.N., Bishop, K., 2012. On the forest cover-water yield debate: From demand- to supply-side thinking. Glob. Chang. Biol. 18, 806–820. https://doi.org/10.1111/j.1365-2486.2011.02589.x.

Francis, T.B., Abbott, K.C., Cuddington, K., Gellner, G., Hastings, A., Lai, Y.C., Morozov, A., Petrovskii, S., Zeeman, M.L., 2021. Management implications of long transients in ecological systems. Nat. Ecol. Evol. 5, 285–294. https://doi.org/10.1038/s41559-020-01365-0.

Fu, B., Wang, S., Su, C., Forsius, M., 2013. Linking ecosystem processes and ecosystem services. Curr. Opin. Environ. Sustain. 5, 4–10. https://doi.org/10.1016/j.cosust.2012.12.002.

Fu, B., Wu, X., Wang, Z., Wu, X., Wang, S., 2022. Coupling Human and Natural Systems for Sustainability: experoence from China's Loess Plateau. Earth Syst. Dynam. 13, 795–808.

Grill, G., Lehner, B., Thieme, M., Geenen, B., Tickner, D., Antonelli, F., Babu, S., Borrelli, P., Cheng, L., Crochetiere, H., Ehalt Macedo, H., Filgueiras, R., Goichot, M., Higgins, J., Hogan, Z., Lip, B., McClain, M.E., Meng, J., Mulligan, M., Nilsson, C., Olden, J.D., Opperman, J.J., Petry, P., Reidy Liermann, C., Sáenz, L., Salinas-Rodríguez, S., Schelle, P., Schmitt, R.J.P., Snider, J., Tan, F., Tockner, K., Valdujo, P. H., van Soesbergen, A., Zarfl, C., 2019. Mapping the world's free-flowing rivers. Nature. 569, 215–221. https://doi.org/10.1038/s41586-019-1111-9.

Hargreaves, G.H., Allen, R.G., 2003. History and evaluation of Hargreaves evapotranspiration equation. J. Irrig. Drain. Eng. 129, 53–63. https://doi.org/10.1061/(ASCE)0733-9437(2003)129:1(53).

Hautier, Y., Tilman, D., Isbell, F., Seabloom, E.W., Borer, E.T., Reich, P.B., 2015. Anthropogenic environmental changes affect ecosystem stability via biodiversity. Science. 348, 336–340. https://doi.org/10.1126/science.aaa1788.

He, D., Wu, S., Peng, H., Yang, Z., Ou, X., Cui, B., 2005. A study of ecosystem changes in longitudinal range-gorge and transboundart eco-security in southwest China. Adv. Earth Sci. 20, 338–344.

He, D., Wu, R., Feng, Y., Li, Y., Ding, C., Wang, W., Yu, D.W., 2014. China's transboundary waters: New paradigms for water and ecological security through applied ecology. J. Appl. Ecol. 51, 1159–1168. https://doi.org/10.1111/1365-2664.12298.

Huo, H., Sun, C., 2021. Spatiotemporal variation and influencing factors of vegetation dynamics based on Geodetector: A case study of the northwestern Yunnan Plateau. China. Ecol. Indic. 130, 108005 https://doi.org/10.1016/j.ecolind.2021.108005.

Jaeger, J.A.G., 2000. Landscape division, splitting index, and effective mesh size: New measures of landscape fragmentation. Landsc. Ecol. 15, 115–130. https://doi.org/10.1023/A:1008129329289.

Jon Paul Rodriguez, 2012. Trade-offs across Space, time, and Ecosystem services. Core Top. Card. Anesth. Second Ed. 345–354 https://doi.org/10.1017/CBO9780511979095.060.

Kéfi, S., Holmgren, M., Scheffer, M., 2016. When can positive interactions cause alternative stable states in ecosystems? Funct. Ecol. 30, 88–97. https://doi.org/10.1111/1365-2435.12601.

Kuri, F., Murwira, A., Murwira, K.S., Masocha, M., 2014. Predicting maize yield in Zimbabwe using dry dekads derived fromremotely sensed vegetation condition index. Int. J. Appl. Earth Obs. Geoinf. 33, 39–46. https://doi.org/10.1016/j.jag.2014.04.021.

Lee, H., Lautenbach, S., 2016. A quantitative review of relationships between ecosystem services. Ecol. Indic. 66, 340–351. https://doi.org/10.1016/j.ecolind.2016.02.004.

Li, Y., Wang, J., Li, Y., 2015. Characteristics of a Regional Meteorological Drought Event in Southwestern China During 2009–2010. J. Arid Meteorol. 33, 537–545. https://doi.org/10.11755/j.issn.1006-7639(2015)-04-0537.

Li, R., Zheng, H., O'Connor, P., Xu, H., Li, Y., Lu, F., Robinson, B.E., Ouyang, Z., Hai, Y., Daily, G.C., 2021. Time and space catch up with restoration programs that ignore ecosystem service trade-offs. Sci. Adv. 7, 1–10. https://doi.org/10.1126/sciadv.abf8650.

Liu, Y.J., Jiang, Y.A., Xu, C., Lyu, J.Y., Su, Z.H., 2022. A quantitative analysis framework for water-food-energy nexus in an agricultural watershed using WEAP-MODFLOW. Sustain. Prod. Consum. 31, 693–706. https://doi.org/10.1016/j.spc.2022.03.032.

Ma, L., Bo, J., Li, X., Fang, F., Cheng, W., 2019. Identifying key landscape pattern indices influencing the ecological security of inland river basin: The middle and lower reaches of Shule River Basin as an example. Sci. Total Environ. 674, 424–438. https://doi.org/10.1016/j.scitotenv.2019.04.107.

Mayer, A.L., Rietkerk, M., 2004. The dynamic regime concept for ecosystem management and restoration. Bioscience. 54, 1013–1020. https://doi.org/10.1641/0006-3568(2004)054[1013:TDRCFE]2.0.CO;2.

McGarigal, L., Marks, B., 1995. FRAGSTATS Manual: spatial pattern analysis program for quantifying landscape structure PNW-GTR-351. Pacific Northwest Research Station, Portland, OR, pp. 122.

Milkoreit, M., Hodbod, J., Baggio, J., Benessaiah, K., Calderón-Contreras, R., Donges, J. F., Mathias, J.D., Rocha, J.C., Schoon, M., Werners, S.E., 2018. Defining tipping points for social-ecological systems scholarship—an interdisciplinary literature review. Environ. Res. Lett. 13 https://doi.org/10.1088/1748-9326/aaaa75.

Mohammadi, M., Darabi, H., Mirchooli, F., Bakhshaee, A., Torabi Haghighi, A., 2021. Flood risk mapping and crop-water loss modeling using water footprint analysis in agricultural watershed, northern Iran. Nat. Hazards. 105, 2007–2025. https://doi.org/10.1007/s11069-020-04387-w.

Möllmann, C., Diekmann, R., Müller-karulis, B., Kornilovs, G., Plikshs, M., Axe, P., 2009. Reorganization of a large marine ecosystem due to atmospheric and anthropogenic pressure: A discontinuous regime shift in the Central Baltic Sea. Glob. Chang. Biol. 15, 1377–1393. https://doi.org/10.1111/j.1365-2486.2008.01814.x.

Mumby, P.J., Chollett, I., Bozec, Y.M., Wolff, N.H., 2014. Ecological resilience, robustness and vulnerability: How do these concepts benefit ecosystem management? Curr. Opin. Environ. Sustain. 7, 22–27. https://doi.org/10.1016/j.cosust.2013.11.021.

Ospina, D., Peterson, G., Crépin, A.S., 2019. Migrant remittances can reduce the potential of local forest transitions—a social-ecological regime shift analysis. Environ. Res. Lett. 14 https://doi.org/10.1088/1748-9326/aaf0ee.

Ouyang, Z., Zheng, H., Xiao, Y.i., Polasky, S., Liu, J., Xu, W., Wang, Q., Zhang, L., Xiao, Y., Rao, E., Jiang, L., Lu, F., Wang, X., Yang, G., Gong, S., Wu, B., Zeng, Y., Yang, W., Daily, G.C., 2016. Improvements in ecosystem services from investments in natural capitall. Science. 352, 1455–1459. https://doi.org/10.1126/science.aaf2295.

Pan, Y., Wu, J., Xu, Z., 2014. Analysis of the tradeoffs between provisioning and regulating services from the perspective of varied share of net primary production in an alpine grassland ecosystem. Ecol. Complex. 17, 79–86. https://doi.org/10.1016/j.ecocom.2013.11.001.

[dataset] Peng, S., 2020a. 1-km monthly minimum temperature dataset for China (1901-2021). Natl. Tibet. Plateau Data Cent. 10.5281/zenodo.3114194.

[dataset] Peng, S., 2020b. 1-km monthly maximum temperature dataset for China (1901-2021). Natl. Tibet. Plateau Data Cent. 10.5281/zenodo.3114194.

[dataset] Peng, S., 2020c. 1-km monthly precipitation dataset for China (1901-2021). Natl. Tibet. Plateau Data Cent. 10.5281/zenodo.3185722.

Pettitt, A.N., 1979. A Non-Parametric Approach to the Change-Point Problem Published by : Wiley for the Royal Statistical Society A Non-parametric Approach to the Change-point Problem. J. R. Stat. Soc. Ser. C. 28, 126–135.

Rietkerk, M., Dekker, S.C., De Ruiter, P.C., Van De Koppel, J., 2004. Self-organized patchiness and catastrophic shifts in ecosystems. Science. 305, 1926–1929. https://doi.org/10.1126/science.1101867.

Rocha, J.C., Peterson, G.D., Biggs, R., 2015. Regime shifts in the anthropocene: Drivers, risks, and resilience. PLoS One. 10, 10–12. https://doi.org/10.1371/journal.pone.0134639.

Sasaki, T., Furukawa, T., Iwasaki, Y., Seto, M., Mori, A.S., 2015. Perspectives for ecosystem management based on ecosystem resilience and ecological thresholds against multiple and stochastic disturbances. Ecol. Indic. 57, 395–408. https://doi.org/10.1016/j.ecolind.2015.05.019.

Scheffer, M., Carpenter, S., Foley, J.A., Folke, C., Walker, B., 2001. Catastrophic shifts in ecosystems. Nature. 413, 591–596.

Scheffer, M., Bascompte, J., Brock, W.A., Brovkin, V., Carpenter, S.R., Dakos, V., Held, H., Van Nes, E.H., Rietkerk, M., Sugihara, G., 2009. Early-warning signals for critical transitions. Nature. 461, 53–59. https://doi.org/10.1038/nature08227.

Scheffer, M., Carpenter, S.R., Lenton, T.M., Bascompte, J., Brock, W., Dakos, V., Van De Koppel, J., Van De Leemput, I.A., Levin, S.A., Van Nes, E.H., Pascual, M., Vandermeer, J., 2012. Anticipating critical transitions. Science. 338, 344–348. https://doi.org/10.1126/science.1225244.

Sharp, R., Tallis, H.T., Ricketts, T., Guerry, A.D., Wood, S.A., Chaplin-Kramer, R., Nelson, E., Ennaanay, D., Wolny, S., Olwero, N., Vigerstol, K., Pennington, D., Mendoza, G., Aukema, J., Foster, J., Forrest, J., Gameron, D., Arkema, K., Lonsdorf, E., Kennedy, C., Verutes, G., Kim, C.K., Guannel, G., Papenfus, M., Toft, J., Mrsik, M., Bernhardt, J., Griffin, R., Glowinski, K., Chaumont, N., Perelman, A., Lacayo, M., Mandle, L., Hamel, P., Vogl, A.L., Rogers, L., Bierbower, W., Denu, D., Douglass, J., 2018. InVEST 3.5.0 user's guide. Stanford University, University of Minnesota, The Nature Conservancy, and World Wildlife Fund.

Su, X., Shen, Y., Xiao, Y., Liu, Y., Cheng, H., Wan, L., Zhou, S., Yang, M., Wang, Q., Liu, G., 2022. Identifying Ecological Security Patterns Based on Ecosystem Services Is a Significative Practice for Sustainable Development in Southwest China. Front. Ecol. Evol. 9, 1–13. https://doi.org/10.3389/fevo.2021.810204.

Suding, K.N., Hobbs, R.J., 2009. Threshold models in restoration and conservation: a developing framework. Trends Ecol. Evol. 24, 271–279. https://doi.org/10.1016/j.tree.2008.11.012.

Terrado, M., Sabater, S., Chaplin-Kramer, B., Mandle, L., Ziv, G., Acuña, V., 2016. Model development for the assessment of terrestrial and aquatic habitat quality in conservation planning. Sci. Total Environ. 540, 63–70. https://doi.org/10.1016/j.scitotenv.2015.03.064.

Tischendorf, L., 2001. Can landscape indices predict ecological processes consistently? Landsc. Ecol. 16, 235–254. https://doi.org/10.1023/A:1011112719782.

Tomczak, M.T., Dinesen, G.E., Hoffmann, E., Maar, M., Støttrup, J.G., 2013a. Integrated trend assessment of ecosystem changes in the Limfjord (Denmark): Evidence of a recent regime shift? Estuar. Coast. Shelf Sci. 117, 178–187. https://doi.org/10.1016/j.ecss.2012.11.009.

Tomczak, M.T., Heymans, J.J., Yletyinen, J., Niiranen, S., Otto, S.A., Blenckner, T., 2013b. Ecological Network Indicators of Ecosystem Status and Change in the Baltic Sea. PLoS One. 8, 1–11. https://doi.org/10.1371/journal.pone.0075439.

Wang, Y., Dai, E., Yin, L., Ma, L., 2018. Land use/land cover change and the effects on ecosystem services in the Hengduan Mountain region. China. Ecosyst. Serv. 34, 55–67. https://doi.org/10.1016/j.ecoser.2018.09.008.

Wei, P., Chen, S., Wu, M., Deng, Y., Xu, H., Jia, Y., Liu, F., 2021. Using the invest model to assess the impacts of climate and land use changes on water yield in the upstream regions of the shule river basin. Water. 13, 1–20. https://doi.org/10.3390/w13091250.

Williams, J.R., Jones, C.A., Dyke, P.T., 1984. A modeling approach to determining the relationship between erosion and soil productivity. Trans. ASAE. 27, 129–144.

Wood, S.L.R., Jones, S.K., Johnson, J.A., Brauman, K.A., Chaplin-kramer, R., Fremier, A., Girvetz, E., Gordon, L.J., Kappel, C.V., Mandle, L., Mulligan, M., Farrell, P.O., Smith, W.K., Willemen, L., Zhang, W., Declerck, F.A., 2018. Distilling the role of ecosystem services in the Sustainable Development Goals. Ecosyst. Serv. 29, 70–82. https://doi.org/10.1016/j.ecoser.2017.10.010.

Wu, J., 2013. Landscape sustainability science: Ecosystem services and human well-being in changing landscapes. Landsc. Ecol. 28, 999–1023. https://doi.org/10.1007/s10980-013-9894-9.

Wu, S., Dai, E., He, D., 2005. Major Research Perspectives on Environmental and Developmental Issues for the Longitudinal Range-Gorge Region (LRGR) in Southwestern China. Prog. Geogr. 24, 31–40.

Wu, X., Wei, Y., Fu, B., Wang, S., Zhao, Y., Moran, E.F., 2020. Evolution and effects of the social-ecological system over a millennium in China's loess plateau. Sci. Adv. 6, 1–11. https://doi.org/10.1126/sciadv.abc0276.

Xu, Z., Peng, J., Qiu, S., Liu, Y., Dong, J., Zhang, H., 2022. Responses of spatial relationships between ecosystem services and the Sustainable Development Goals to urbanization. Sci. Total Environ. 850, 157868 https://doi.org/10.1016/j.scitotenv.2022.157868.

Yang, S., Bai, Y., Alatalo, J.M., Wang, H., Jiang, B., Liu, G., Chen, J., 2021b. Spatio-temporal changes in water-related ecosystem services provision and trade-offs with food production. J. Clean. Prod. 286, 125316 https://doi.org/10.1016/j.jclepro.2020.125316.

Yang, F., Lu, H., Yang, K., Huang, G. wei, Li, Y. shan, Wang, W., Lu, P., Tian, F. qiang, Huang, Y. gang, 2021. Hydrological characteristics and changes in the Nu-Salween River basin revealed with model-based reconstructed data. J. Mt. Sci. 18, 2982–3002. 10.1007/s11629-021-6727-1.

Yang, J., Huang, X., 2021. The 30 m annual land cover dataset and its dynamics in China from 1990 to 2019. Earth Syst. Sci. Data. 13, 3907–3925. https://doi.org/10.5194/essd-13-3907-2021.

Yang, W., Jin, Y., Sun, T., Yang, Z., Cai, Y., Yi, Y., 2018. Trade-offs among ecosystem services in coastal wetlands under the effects of reclamation activities. Ecol. Indic. 92, 354–366. https://doi.org/10.1016/j.ecolind.2017.05.005.

Yang, S., Zhao, W., Liu, Y., Cherubini, F., Fu, B., Pereira, P., 2020. Prioritizing sustainable development goals and linking them to ecosystem services: A global expert's knowledge evaluation. Geogr. Sustain. 1, 321–330. https://doi.org/10.1016/j.geosus.2020.09.004.

Yohannes, H., Soromessa, T., Argaw, M., Dewan, A., 2021. Impact of landscape pattern changes on hydrological ecosystem services in the Beressa watershed of the Blue Nile Basin in Ethiopia. Sci. Total Environ. 793, 148559 https://doi.org/10.1016/j.scitotenv.2021.148559.

Yu, Y., Pan, F., Liu, X., Chen, W., He, D., 2017. Variations and trends of trans-boundary runoff in the longitudinal range-gorge region. J. Mt. Sci. 14, 316–324. https://doi.org/10.1007/s11629-016-3862-1.

Yu, Y., Sun, X., Wang, J., Zhang, J., 2022. Using InVEST to evaluate water yield services in Shangri-La, Northwestern Yunnan. China. PeerJ. 10, 1–21. https://doi.org/10.7717/peerj.12804.

Zhang, K., Dearing, J.A., Dawson, T.P., Dong, X., Yang, X., Zhang, W., 2015. Poverty alleviation strategies in eastern China lead to critical ecological dynamics. Sci. Total Environ. 506–507, 164–181. https://doi.org/10.1016/j.scitotenv.2014.10.096.

Zhou, R., Lin, M., Gong, J., Wu, Z., 2019. Spatiotemporal heterogeneity and influencing mechanism of ecosystem services in the Pearl River Delta from the perspective of LUCC. J. Geogr. Sci. 29, 831–845. https://doi.org/10.1007/s11442-019-1631-0.

Zhou, W., Liu, G., Pan, J., 2005. Distribution of available soil water capacity in China. J. Geogr. Sci. 15, 3–12. https://doi.org/10.1360/gs050101.

Zhou, Y., Shi, C., Fan, X., Du, J., 2011. Advances in the Research Methods of Abrupt Changes of Hydrologic Sequences and Their Applications in Drainage Basins in China. Prog. Geogr. 30, 1361–1369.